ISBN: 978-3-95450-234-9 ISSN: 2673-5504 doi:10.18429/JACoW-SRF2023-WEPWB065

IMPACT OF MEDIUM TEMPERATURE HEAT TREATMENTS ON THE MAGNETIC FLUX EXPULSION BEHAVIOR OF SRF CAVITIES*

J. C. Wolff[1,†], J. Eschke, A. Goessel, K. Kasprzak, D. Reschke, L. Steder, L. Trelle, M. Wiencek
Deutsches Elektronen-Synchrotron DESY, Hamburg, Germany
W. C. A. Hillert, University of Hamburg, Germany
[1]also at University of Hamburg, Germany

Abstract

Medium temperature (mid-T) heat treatments at about 300 °C are used to enhance the intrinsic quality factor of superconducting radio frequency (SRF) cavities. Unfortunately, such treatments potentially increase the sensitivity to trapped magnetic flux and consequently the surface resistance of the cavity. For this reason, it is crucial to maximize the expulsion of magnetic flux during the cool down. The flux expulsion behavior is next to the heat treatment mainly determined by the geometry, the niobium grain size and the grain orientation. However, it is also affected by parameters of the cavity performance tests like the cool down velocity, the spatial temperature gradient along the cavity surface and the magnetic flux density during the transition of the critical temperature.

To improve the flux expulsion behavior and hence the efficiency of future accelerator facilities, the impact of these adjustable parameters as well as the mid-T heat treatment on 1.3 GHz TESLA-Type single-cell cavities is investigated by a new approach of a magnetometric mapping system. In this contribution first performance test results of cavities before- and after mid-T heat treatment are presented.

INTRODUCTION

Close to the transition temperature T_c of a type II superconductor (e.g. niobium) the critical magnetic field is strongly suppressed and can fall below the ambient magnetic field [1]. In this case magnetic flux vortices penetrating the bulk are trapped in so-called pinning centers even if the Meissner region is reached. This effect is enhanced by imperfections of the crystal lattice like material impurities, dislocations and grain boundaries [2]. Since these pinning centers remain normal conducting in the Meissner region, they have a significant negative impact on the surface resistance R_s given by:

$$R_s = R_{BCS} + R_{res} + R_{flux} \quad (1)$$

and consequently on the intrinsic quality factor Q_0 [3]. Here R_{BCS} represents the temperature dependent contribution described by the Bardeen Cooper Schrieffer (BCS) theory, R_{res} the constant residual resistance and R_{flux} the impact by the normal conducting pinning centers with a linear dependence of the ambient magnetic field [2, 3]. Studies by [1, 2, 4, 5] have shown that the amount of trapped magnetic flux is influenced by the cool down velocity and the spatial temperature gradient. At least at the first glance these works resulted in contradictory conclusions concerning these two cool down dynamics. Studies at Helmholtz Zentrum Berlin (HZB) presented in Ref. [2] observed the presence of thermoelectric fields and a related inherent trapping of magnetic flux for cavities dressed by a helium tank made of titanium. Since the responsible thermoelectric voltage (Seebeck effect) rises for larger spatial temperature gradients, an increased R_{flux} was observed during subsequent studies using a sample-based setup in an ambient field below 50 nT. During these studies a larger cool down velocity at the T_c transition led to a greater suppression of the Meissner effect.

A similar setup at HZB presented in Ref. [4] is operated in an ambient field of up to $\pm$ 200 µT. At these fields a positive impact of larger spatial temperature gradients at the T_c transition could be shown and a temperature gradient dependent threshold which needs to be reached before any flux trapping could be measured was reported.

Contrary to these reports, colleagues at Fermi National Accelerator Laboratory (FNAL) observed a positive impact of a larger cool down velocity during cavity studies [5] which was explained by different cool down procedures. To achieve the high cool down velocity, the cryostat was filled with liquid helium resulting in a well defined T_c transition from the bottom of the cavity to the top. However, to perform the slow cool down a controlled mixture of warm- and liquid helium was used. This slow cool down method potentially resulted in the formation of normal conducting "islands" enclosed by superconducting material and consequently in an increase of trapped magnetic flux.

Based on these former investigations the impact of the cool down velocity and the temperature gradient can be summarized as follows. In general, a slower cool down velocity seems to be beneficial for a greater expulsion of magnetic flux. Indeed, the formation of normal conducting "islands" enclosed by superconducting material during the cool down should be avoided by choosing an appropriate cool down procedure.

The impact of the temperature gradient is strongly dependent on the ambient conditions. If the experimental setup enables the generation of thermoelectric currents, a larger temperature gradient potentially affects the cavity performance due to the related inherent trapping of magnetic flux. Exemplary this can be the case for a dressed cavity in a

* This work was supported by the Helmholtz Association within the topic Accelerator Research and Development (ARD) of the Matter and Technologies (MT) Program.
† Jonas.Wolff@desy.de

ISBN: 978-3-95450-234-9 ISSN: 2673-5504 doi:10.18429/JACoW-SRF2023-WEPWB065

low field environment. However, a high spatial temperature gradient enhances the expulsion of external magnetic flux. Consequently, as long as the impact of inherent trapped flux related to thermoelectric currents is smaller than the impact of the external flux which would be trapped in case of a smaller temperature gradient, high temperature gradients can be beneficial for the general flux expulsion and hence for the cavity performance.

For test comprehensive comparisons, commonly the ratio of the magnetic flux density in superconducting state B_{sc} and the magnetic flux density in normal conducting state B_{nc} measured at the equator position is used [5]. Based on a simulation model the extremum of the ideal Meissner state can be obtained and the percental fraction of the magnetic flux trapped in the bulk material can be derived [5]. In case of the DESY setup an increase of the magnetic flux density in the ideal Meissner state by a factor of 1.65 was obtained by a SIMULIA CST Studio Suite model.

The impact of the trapped magnetic flux on the surface resistance depends, next to the fraction trapped, also on the penetration depth of the RF field and hence on the electron mean free path l. Consequently, ultra high vacuum (UHV) cavity heat treatments may have an impact on the sensitivity to trapped magnetic flux S. Here, S is given by:

$$S = \frac{\Delta R_s}{B_{trap}}, \tag{2}$$

where ΔR_s depicts the increase of R_s per unit of trapped magnetic flux B_{trap} [6].

Mid-T heat treatments like the in-situ "mid-T bake" of FNAL described in Ref. [7] based on the work of [8] and the variant of the High Energy Accelerator Research Organisation (KEK) "mid-T furnace baking" [6] exposing the inner cavity surface to air after surface treatment showed high Q_0 of up to $5 \cdot 10^{10}$ at 2 K and quench fields between 20 - 37 MV/m [6, 7, 9], but an increased S was observed at both, FNAL and KEK [6, 7].

In this contribution the flux expulsion behavior will be separately investigated as a function of the cool down velocity and the spatial temperature gradient for the large-grain single-cell cavity 1DE26 before- and after mid-T heat treatment (280 °C; 3 h) performed in the DESY niobium retort UHV furnace as described in Ref. [10]. Furthermore, a potential impact of the mid-T heat treatment on the sensitivity to trapped magnetic flux will be studied. To distinguish between asymmetries of the flux expulsion behavior related to the large-grain material and potential anomalies caused by an inhomogeneous helium flow during the cool down all tests were repeated with the fine-grain cavity 1DE09 after mid-T heat treatment (300 °C; 3 h) for comparison.

EXPERIMENTAL SETUP

For the related studies the finalized magnetometric mapping system shown in Fig. 1, based on the work of [11, 12] and introduced in Ref. [13, 14] is used instead of a single magnetometer mounted at the equator. This enables to a

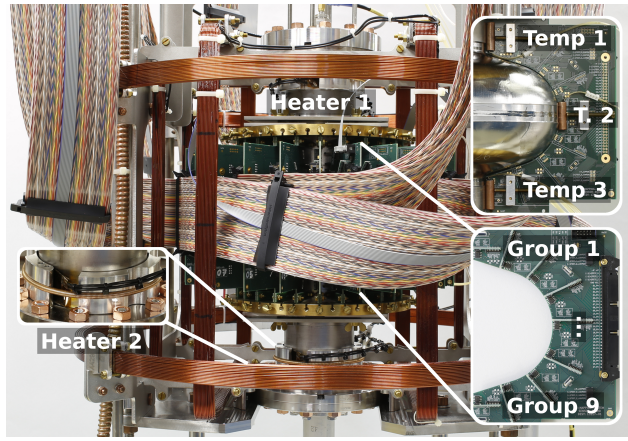

(a)

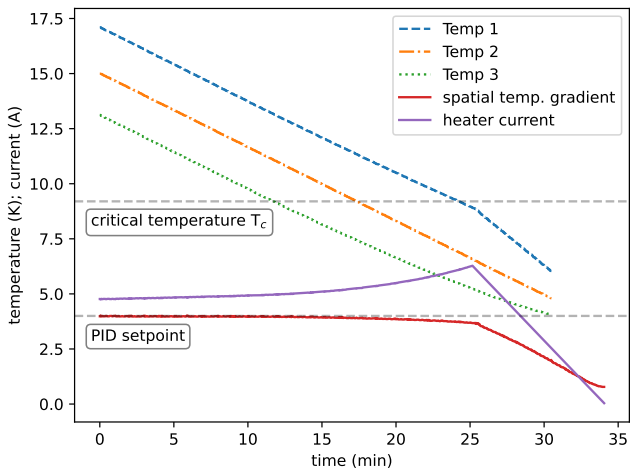

(b)

Figure 1: Experimental setup: Cavity 1DE26 surrounded by 23 sensor boards and one board for the thermocouples to control the cool down velocity (Temp 2(T. 2)) and the spatial temperature gradient defined as (Temp 1 - Temp 3)/Δl where Δl represents the distance between Temp 1 and Temp 3 along the surface of 225 mm (a). PID-controlled spatial temperature gradient as a function of the time for a cool down velocity of −20 K/h and a spatial temperature gradient of 4 ΔK/Δl (b).

certain degree the detection of grain boundary dependent differences in the flux expulsion behavior and the potential formation of normal conducting "islands" [5]. Furthermore, the spatial T_c transition along the cavity surface and hence anomalies of the cool down can be monitored. To study the impact of the cool down velocity, each (linear) cool down is performed as follows. Since the permeability of the cryostats magnetic shielding (and consequently the ambient field) is temperature dependent, the cryostat is filled with liquid helium to a defined maximum level before each test to ensure test comprehensive consistent conditions for the ambient magnetic field. At a helium bath temperature of 2 K the liquid helium level is lowered below the experimental setup. Afterwards the pressure is PID-controlled reduced until a target temperature of 3 K is reached using the

ISBN: 978-3-95450-234-9 ISSN: 2673-5504 doi:10.18429/JACoW-SRF2023-WEPWB065

equator thermocouple Temp 2 shown in Fig. 1 as reference. However, a change of the cool down velocity will affect the spatial temperature gradient and consequently hamper a later classification of the impact on the magnetic flux trapping behavior of each adjustable parameter. For this reason, the temperature gradient is controlled by two heaters. Each of these heaters consists of two heating tapes of type Conflux P46035-A mounted on both drift tubes by custom-built holders. Due to their low residual resistance at cryogenic temperatures unfortunately a comparatively high heater current of several Ampere is required to drive the needed power to the cavity. To minimize the stray impact of the magnetic flux related to this current, the supply lines are conducted as a twin line and the heaters are mounted with a large distance to the cavity cell next to the cavity flanges. Both heaters are controlled by a PID-loop using two Cryotronics CERNOX CX1030 thermocouples (Temp 1 and Temp 3) located at the upper- and lower iris as reference. The loop parameters were manually adjusted until satisfactory results could be achieved.

Indeed, divergent to initial expectations an inclined T_c transition was noticed by an evaluation of the flux density snapshots as a function of the time. One is exemplary shown in Fig. 2. This inclined T_c transition is likely caused by an inhomogeneous helium gas flow due to asymmetrical steel plates below the experimental setup partly visible at the bottom of Fig. 1. The given numbers next to some of the shown vector arrows indicate the expulsion ratio $|B_{sc}/B_{nc}|$. A ratio $|B_{sc}/B_{nc}| < 1$ is caused by a partial shielding of magnetic flux due to nearby superconducting material.

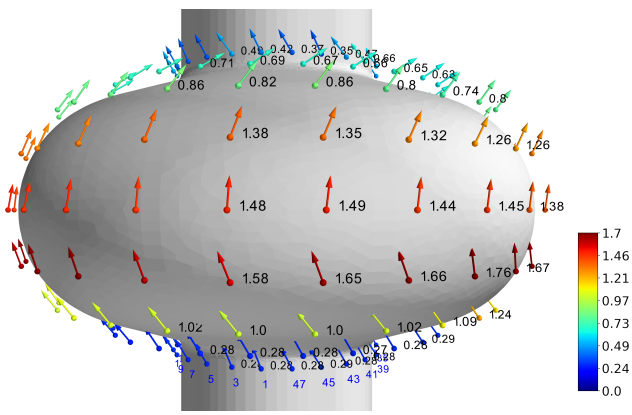

Figure 2: Magnetic flux distribution snapshot of the cavity 1DE26 recorded before mid-T heat treatment in superconducting state for a cool down velocity of −5 K/h and a spatial temperature gradient of 4 $\Delta K/\Delta l$. The given numbers indicate the expulsion ratio $|B_{sc}/B_{nc}|$. An inclined T_c transition led to an asymmetrical magnetic flux expulsion. The reversed orientation of the Group 1 vector arrows was caused by the heater current.

To independently investigate the impact of the cool down velocity and the spatial temperature gradient on the flux expulsion behavior, the related test series were carried out under the following conditions. For the cool down dynamics assumed technical extrema of −5 K/h and −20 K/h for the cool down velocity as well as 0 $\Delta K/\Delta l$ and 4 $\Delta K/\Delta l$ (where Δl represents the distance between Temp 1 and Temp 3 along the cavity surface of about 225 mm) for the spatial temperature gradient were chosen to maximize the likelihood of significant measurement results. During each measurement series a separate cool down for each possible combination of these assumed technical extrema was performed. For all controlled cool downs presented in this contribution a defined magnetic stray field of 10 µT was applied in vertical direction by the respective Helmholtz coil. Every cool down was followed by at least two vertical performance tests at 2 K to evaluate the surface resistance R_s and hence the sensitivity to trapped magnetic flux S.

RESULTS

The polar distribution of the ratio $|B_{sc}/B_{nc}|$ is shown in Fig. 3 separately for each sensor group as a function of the cool down dynamics for all cool downs of the 1DE26 and 1DE09 test series to illustrate the magnetic flux expulsion behavior. Except for the 1DE26 dataset recorded before mid-T heat treatment at −20 K/h and 0 $\Delta K/\Delta l$, no significant differences in the flux expulsion behavior could be observed for the two chosen cool down velocities. Furthermore, no additional changes of the flux expulsion potentially linked to the mid-T heat treatment could be measured. The low flux expulsion of this dataset was likely caused by a different initial liquid helium level in the cryostat and a consequently lower real temperature gradient in between the two reference thermocouples Temp 1 and Temp 3. Indeed, a large dependence of the used spatial temperature gradient could be observed. The best mean expulsion ratios of 1.45 in case of 1DE26 and 1.22 for 1DE09 could be achieved for the high temperature gradient of 4 $\Delta K/\Delta l$. Divergent to the fraction of trapped magnetic flux, the surface resistance R_s shown in Fig. 4 as a function of the effective accelerating gradient E_{acc} increased in all cases after the mid-T heat treatment except for the baseline measurements. The resulting sensitivity to trapped magnetic flux increased by a factor of five from 3.1 nΩ/µT to 15.7 nΩ/µT in case of the higher temperature gradient and from 3.5 nΩ/µT to 17.7 nΩ/µT for the lower temperature gradient after mid-T heat treatment.

CONCLUSION

The impact of the cool down velocity and the spatial temperature gradient on the flux expulsion behavior of 1.3 GHz TESLA-Type single-cell SRF cavities was separately investigated by a magnetometric mapping system. To maximize the likelihood of significant measurement results, assumed technical extrema of −5 K/h and −20 K/h for the cool down velocity as well as 0 $\Delta K/\Delta l$ and 4 $\Delta K/\Delta l$ (where Δl describes the distance between two reference thermocouples mounted at the upper- and lower iris of about 225 mm) for the spatial temperature gradient were used. The magnetic flux expulsion behavior during the T_c transition was measured for each possible combination of these technical extrema. A respec-

ISBN: 978-3-95450-234-9 ISSN: 2673-5504 doi:10.18429/JACoW-SRF2023-WEPWB065

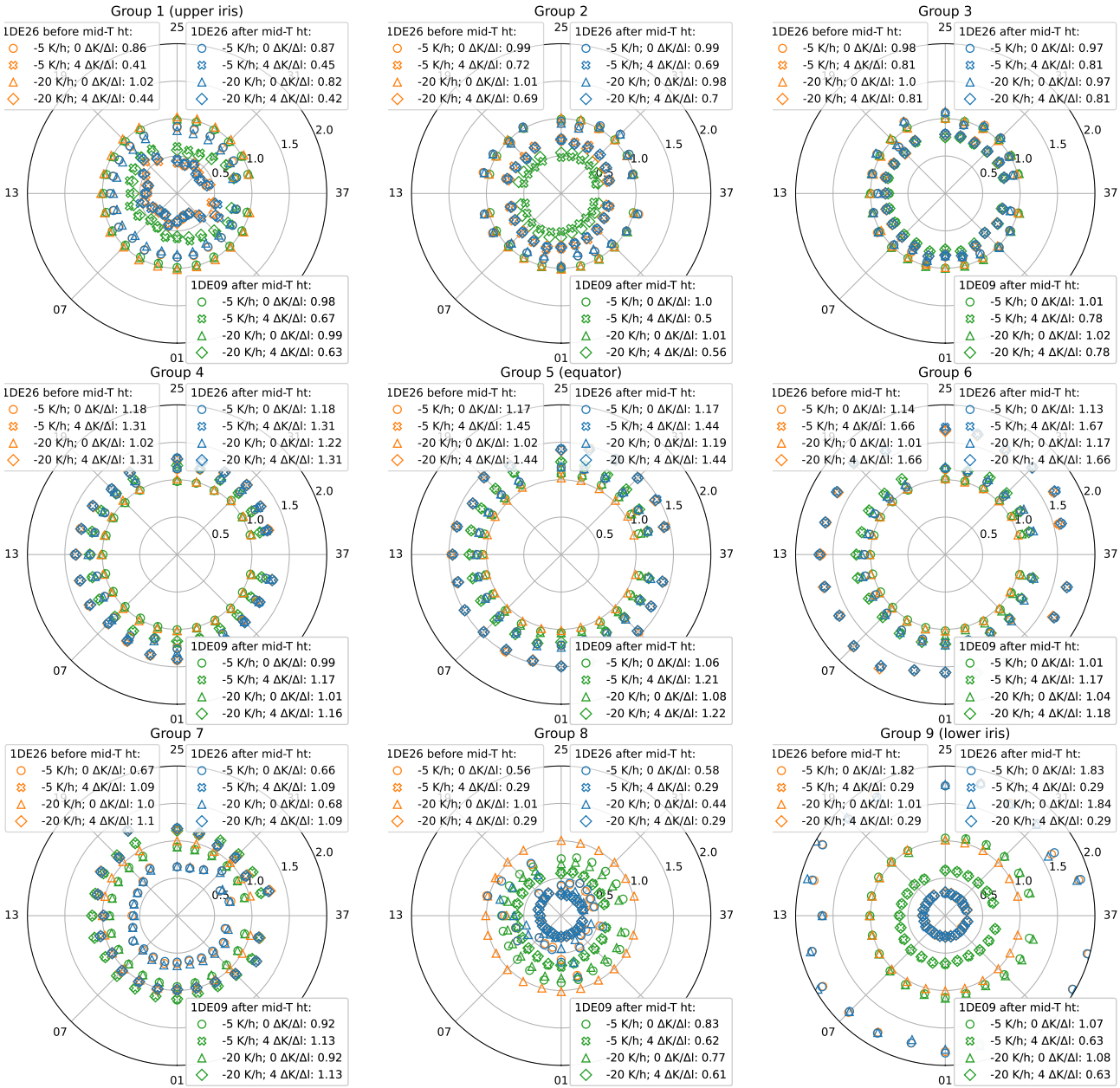

Figure 3: Polar distribution of the ratio $|B_{sc}/B_{nc}|$ separately for each sensor group shown in Fig. 1 as a function of the cool down velocity and the temperature gradient at an ambient field of 10 µT in vertical direction before- and after mid-T heat treatment (mid-T ht) to illustrate the magnetic flux expulsion behavior of the large-grain cavity 1DE26. The results of the fine-grain cavity 1DE09 after mid-T heat treatment are shown for comparison to distinguish between asymmetries of the flux expulsion behavior related to the large-grain material and potential anomalies caused by an inhomogeneous helium flow. The θ-labels indicate the card identifier of each sensor board (01-47).

tive cool down series was carried out for the large-grain cavity 1DE26 before- and after mid-T heat treatment. Each cool down was followed by a vertical performance test at 2 K to evaluate the impact on the surface resistance and hence the sensitivity to trapped magnetic flux. One complete test series was repeated with the fine-grain cavity 1DE09 after mid-T heat treatment to distinguish between asymmetries of the flux expulsion behavior related to the large-grain material and potential anomalies caused by a inhomogeneous helium flow during the cool down.

Except for the 1DE26 dataset recorded before mid-T heat treatment at a cool down velocity of −20 K/h and a spatial temperature gradient of 0 $\Delta K/\Delta l$ no significant changes in the flux expulsion behavior related to the cool down velocity or the mid-T heat treatment could be measured. The deviant behavior of this dataset was likely caused by a different initial liquid helium level before the start of the respective cool down and a consequently lower real temperature gradient between the two reference thermocouples. However, an extensive dependence of the used spatial temperature

ISBN: 978-3-95450-234-9 ISSN: 2673-5504 doi:10.18429/JACoW-SRF2023-WEPWB065

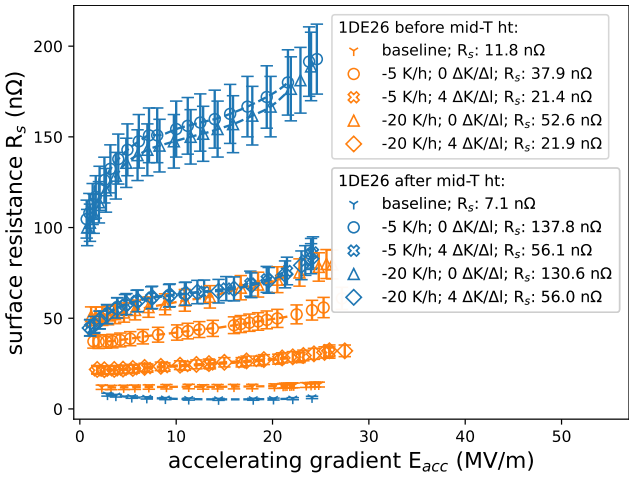

Figure 4: Surface resistance R_s as a function of the accelerating gradient E_{acc} of cavity 1DE26 before- and after mid-T heat treatment (mid-T ht) recorded at 2 K with an applied magnetic stray flux density of 10 µT. The surface resistance R_s given in the legend was obtained by cubic interpolation for an accelerating gradient E_{acc} of 4 MV/m. Both baseline curves were recorded according to the common test procedure without an applied magnetic stray field.

gradient on the flux expulsion behavior of both test cavities could be observed. Here, a higher temperature gradient was linked to an improved expulsion of magnetic flux in all cases. By taking the characteristics of the experimental setup like the comparatively high ohmic loop resistance of the cavity support structure and the applied magnetic stray field into account, these results are in good agreement with the former studies. The sensitivity to trapped magnetic flux increased by a factor of five from 3.1 nΩ/µT to 15.7 nΩ/µT in case of the higher temperature gradient and from 3.5 nΩ/µT to 17.7 nΩ/µT for the lower temperature gradient after mid-T heat treatment. Consequently, only the sensitivity to trapped magnetic flux increases due to the heat treatment and the flux expulsion behavior remains likely unaffected.

ACKNOWLEDGEMENTS

We would like to thank our colleagues - F. Kramer and O. Kugeler from Helmholtz-Zentrum Berlin, I. Flick, R. Ghanbari, I. Gonzalez Diaz-Palacio, S. Harder, G. Kacha Deyu, C. Saribal and M. Wenskat from University of Hamburg as well as the DESY groups MDI, MKS1, MSL and ZE - for their support of this work.

REFERENCES

[1] T. Kubo, "Flux trapping in superconducting accelerating cavities during cooling down with a spatial temperature gradient," *Prog. Theor. Exp. Phys.*, vol. 2016, no. 5, 053G01, 2016. doi:10.1093/ptep/ptw049

[2] J.-M. Vogt, O. Kugeler, and J. Knobloch, "Impact of cool-down conditions at Tc on the superconducting rf cavity quality factor," *Phys. Rev. Spec. Top. Accel. Beams*, vol. 16, p. 102 002, 2013. doi:10.1103/PhysRevSTAB.16.102002

[3] S. Aull, O. Kugeler, and J. Knobloch, "Trapped magnetic flux in superconducting niobium samples," *Phys. Rev. Spec. Top. Accel. Beams*, vol. 15, no. 6, p. 062 001, 2012. doi:10.1103/PhysRevSTAB.15.062001

[4] F. Kramer, S. Keckert, J. Knobloch, and O. Kugeler, "Systematic Investigation of Flux Trapping Dynamics in Niobium Samples," in *Proc. IPAC'22*, Bangkok, Thailand, 2022, pp. 1200–1203. doi:10.18429/JACoW-IPAC2022-TUPOTK006

[5] A. Romanenko, A. Grassellino, O. Melnychuk, and D. A. Sergatskov, "Dependence of the residual surface resistance of superconducting radio frequency cavities on the cooling dynamics around Tc," *J. Appl. Phys.*, vol. 115, no. 18, 2014, 184903. doi:10.1063/1.4875655

[6] H. Ito, H. Araki, K. Takahashi, and K. Umemori, "Influence of furnace baking on Q–E behavior of superconducting accelerating cavities," *Prog. Theor. Exp. Phys.*, vol. 2021, no. 7, 2021, 071G01. doi:10.1093/ptep/ptab056

[7] S. Posen, A. Romanenko, A. Grassellino, O. Melnychuk, and D. Sergatskov, "Ultralow Surface Resistance via Vacuum Heat Treatment of Superconducting Radio-Frequency Cavities," *Phys. Rev. Appl.*, vol. 13, no. 1, p. 014 024, 2020. doi:10.1103/PhysRevApplied.13.014024

[8] F. Palmer, "Influence of oxide layers on the microwave surface resistance of niobium," *IEEE Trans. Magn.*, vol. 23, no. 2, pp. 1617–1619, 1987. doi:10.1109/TMAG.1987.1064847

[9] F. He *et al.*, "Medium-temperature furnace bake of Superconducting Radio-Frequency cavities at IHEP," 2020. doi:10.48550/arXiv.2012.04817

[10] L. Trelle *et al.*, "Refurbishment and Reactivation of a Niobium Retort Furnace at DESY," presented at SRF'23, Grand Rapids, MI, USA, Jun. 2023, paper TUPTB037, this conference.

[11] B. Schmitz, J. Köszegi, K. Alomari, O. Kugeler, and J. Knobloch, "Magnetometric Mapping of Superconducting RF Cavities," *Rev. Sci. Instrum.*, vol. 89, 2018. doi:10.1063/1.5030509

[12] F. Kramer, O. Kugeler, J.-M. Köszegi, and J. Knobloch, "Impact of geometry on flux trapping and the related surface resistance in a superconducting cavity," *Phys. Rev. Accel. Beams*, vol. 23, no. 12, p. 123 101, 2020. doi:10.1103/PhysRevAccelBeams.23.123101

[13] J. Wolff *et al.*, "Development of a New B-Mapping System for SRF Cavity Vertical Tests," in *Proc. SRF'21*, East Lansing, MI, USA, 2022, pp. 137–141. doi:10.18429/JACoW-SRF2021-SUPTEV009

[14] J. Wolff *et al.*, "Commissioning of a New Magnetometric Mapping System for SRF Cavity Performance Tests," in *Proc. IPAC'22*, Bangkok, Thailand, 2022, pp. 1215–1218. doi:10.18429/JACoW-IPAC2022-TUPOTK011